Available online at www.sciencedirect.com

ScienceDirect

IFAC PapersOnline CONFERENCE PAPER ARCHIVE

IFAC PapersOnLine 54-2 (2021) 114–120

Performance Assessment of Different Cell-Transmission Models for Ramp-Metered Highway Networks

Fatemeh Alimardani * **John S. Baras** *

* *Institute for Systems Research, Department of Electrical & Computer Engineering, University of Maryland, College Park, MD 20742, USA, (email: fatimalm@umd.edu, baras@umd.edu)*

Abstract: Throughout the past three decades, various versions of the the cell-transmission model (CTM) has been proposed. In spite of the increased attention to freeway traffic modelling via the CTM, an analysis of the currently available versions of the CTM has been missing. This study has the aim of filling this gap by comparing the performance of the popular versions of this model. To achieve this goal, four finite horizon optimal control problems with different underlying CTMs and cost functions are proposed. The traffic management control in all problems is the ramp metering control. The performance assessment is performed via simulation for a hypothetical network of highways, with different demand profiles along with the analysis of the equilibrium state in each case. The simulation results will provide a thorough comparison of the performance of these problems on different performance measures of the network and will highlight the advantages and disadvantages of each problem.

Keywords: Cell-transmission model; Traffic flow; Highway networks; Ramp metering, Modeling and simulation of transportation systems, Traffic control systems

1. INTRODUCTION

Traffic flow models have been developed over the years and it is still an ongoing research topic in this field. Traffic flow models can be categorized into first order and second order models. The most frequently used models are first order models, such as the LWR model offered by Lighthill and Whitham (1955), which is a continuous model, and the cell-transmission model (CTM) offered by Daganzo (1993, 1994) which is a discretized version of the LWR model. The focus of this study is on first order models as the obvious disadvantage to second order models is that they lead to more complex optimization problems.

The CTM was first developed by Daganzo (1993) and then, through out the following years, many extensions of the original CTM have been proposed in the literature based on the applications and the purposes of researchers. The CTM for a freeway network (Daganzo (1995)), the lagged CTM (Daganzo (1999); Szeto (2008)), the switched interpretation of the CTM (Muñoz et al. (2003)), the asymmetric CTM (Gomes and Horowitz (2006)), the link-node CTM (Muralidharan et al. (2009)), the CTM including capacity drop phenomena (Srivastava and Geroliminis (2013); Roncoli et al. (2015)), the graph constrained CTM (Morbidi et al. (2014)), the CTM in a mixed-integer linear form (Ferrara et al. (2015)), the variable-length CTM (Canudas-de Wit and Ferrara (2016)), width-based CTM for heterogeneous and undisciplined traffic streams (Ahmed et al. (2019)), CTM for mixed traffic flow with connected and autonomous vehicles (Qin and Wang (2019)), the CTM for heterogeneous disordered traffic (Mayakuntla and Verma (2019)), and multi-class CTM different traffic flow parameters (Chen et al. (2020)) are some of these extended versions. Although these models have been proposed in different years and are suitable for different networks and applications, but still the original CTM Daganzo (1993), and most specifically the Asymmetric CTM (ACTM) Gomes and Horowitz (2006) is the underlying model in all of them. This study aims at the comparison of the most commonly-used versions of the CTM.

The paper is organized as follows: In Section 2, the different versions of the CTM considered here are introduced. In Section 3, the RM control strategy used as the underlying traffic control strategy for the finite horizon optimal control problems (FHOCPs) of this study is briefly explained. The formulation of the FHOCPs are explained in Section 4 and in Section 5 the simulation results are reported and analysed in detail. Finally, some conclusive remarks are drawn in Section 6.

2. THE CTM AND ITS EXTENSIONS

In this section, first, a famous variant of the CTM, called the Asymmetric CTM (ACTM) will be presented which was offered by Gomes and Horowitz (2006). Then, two of the most commonly-used extensions of the ACTM will be introduced which are called the linear relaxation of ACTM (Gomes and Horowitz (2006)) and the extended ACTM (Ferrara et al. (2018)). As ACTM is the core of the other extensions, it won't be evaluated separately and the focus of this study, from now on, will be on performance

⋆ This work was partially supported by ONR grant N00014-17-1-2622, and by DARPA under Agreement No. HR00111990027.

10.1016/j.ifacol.2021.06.016

assessment of the two latter versions of the ACTM. Fig. 1 shows a stretch of a freeway with queue length dynamics borrowed from Ferrara et al. (2015). The variables and parameters of cell i during time interval $[kT, (k+1)T)$ are described in table 1.

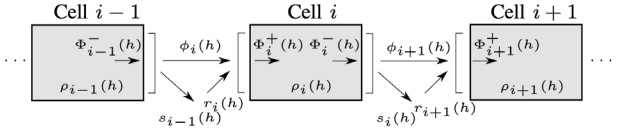

Fig. 1. Sketch of a freeway stretch in the CTM (Ferrara et al. (2015))

Table 1. Model Variables and Parameters

Symbol	Description/Unit (Range)
N	Number of cells / int
i	Cell index / $i = \{1, ..., N\}$
T	Sampling period / (h)
K	Time Horizon / int
k	Time index / $k = \{0, ..., K-1\}$
L_i	Length of each cell / (mi)
v_i	Free-flow speed of cell i / (mi/h)
w_i	Congestion wave speed / (mi/h)
q_i^{max}	Cell capacity / (veh/h)
λ_i	Lane numbers / int
ρ_i^{max}	Jam density / (veh/mi)
ρ_i^{cr}	Critical density / (veh/mi)
l_i^{max}	Maximum on-ramp queue length / (veh/h)
$r_i^{C,max}$	Maximum metering rate / (veh/h)
$\rho_i(k)$	Traffic density / (veh/mi)
$\Phi_i^+(k)$	Total flow entering cell i / (veh/h)
$\Phi_i^-(k)$	Total flow exiting cell i/ (veh/h)
$\phi_i(k)$	Mainstream flow / (veh/h)
$r_i(k)$	Flow entering from the on-ramp / (veh/mi)
$s_i(k)$	Flow exiting through the off-ramp / (veh/mi)
$\beta_i(k)$	Split ratio / $\in [0, 1]$
$l_i(k)$	Queue length in the on-ramp /(veh)
$d_i(k)$	Flow accessing the on-ramp / (veh/h)
$r_i^C(k)$	Ramp metering control variable / (veh/h)
r_i^*	Ramp metering set point / (veh/h)
K_R	Integral regulator gain
K_P	Proportional regulator gain

Version 1: The Asymmetric CTM (ACTM) The ACTM proposed in Gomes and Horowitz (2006), is a modification of the standard CTM proposed by Daganzo (1993, 1994, 1995). Based on Gomes and Horowitz (2006), the relevant difference between the two models is the treatment of traffic merges. More specifically, merges in the ACTM are considered as asymmetric connections, such as the junctions of the on-ramps into the mainstream. According to the logic of the standard CTM, the merge is oriented to move as much of the demand as possible from the two merging cells into the receiving cell. The ACTM, instead, makes separate allocations of supply for each merging flow. The flows can then be computed separately as the minimum among the demand, the allocated supply, and the capacity. Moreover, it is proved that the ACTM, as the CTM, ensures not to predict unrealistic behaviours such as backward moving traffic, negative densities and densities exceeding the jam density.
The ACTM is characterised by the following equations:

$$\rho_i(k+1) = \rho_i(k) + \frac{T}{L}(\Phi_i^+(k) - \Phi_i^-(k)) \tag{1}$$

$$\Phi_i^+(k) = \phi_i(k) + r_i(k) \tag{2}$$

$$\Phi_i^-(k) = \phi_{i+1}(k) + s_i(k) \tag{3}$$

$$s_i(k) = \frac{\beta_i(k)}{1-\beta_i(k)}\phi_{i+1}(k) \tag{4}$$

$$l_i(k+1) = l_i(k) + T(d_i(k) - r_i(k)) \tag{5}$$

$$\phi_i(k) = \min\{(1-\beta_{i-1}(k))v_{i-1}(\rho_{i-1}(k) + r_{i-1}(k)), w_i(\rho_i^{max} - \rho_i(k) - r_i(k)), q_{i-1}^{max}\} \tag{6}$$

For uncontrolled on-ramps:

$$r_i(k) = \min\{l_i(k) + d_i(k), \rho_i^{max} - \rho_i(k)\} \tag{7}$$

For controlled on-ramps:

$$r_i(k) = \min\{l_i(k) + d_i(k), \rho_i^{max} - \rho_i(k), r_i^{C,max}\} \tag{8}$$

$$0 \le \rho_i(k) \le \rho_i^{max}(k) \tag{9}$$

$$0 \le \phi_i(k) \le q_i^{max}(k) \tag{10}$$

$$0 \le r_i(k) \le r_i^{C,max} \tag{11}$$

$$0 \le l_i(k) \le l_i^{max} \tag{12}$$

Equations (1) through (12) describe the ACTM. Any optimization formulation based on this model will be non-concave and non-convex due to the *min* function in the mainline and on-ramp flow equations in (6)-(8).

Version 2: Linear Relaxation of ACTM Gomes and Horowitz (2006) offered this linear relaxed version of ACTM where (6)-(8) are replaced with linear equality and inequality equations and also upper bounds.
Equation (6) is replaced with:

$$\phi_i(k) \le (1-\beta_{i-1}(k))v_{i-1}(\rho_{i-1}(k) + r_{i-1}(k)) \tag{13}$$

$$\phi_i(k) \le w_i(\rho_i^{max} - \rho_i(k) - r_i(k)) \tag{14}$$

$$\phi_i(k) \le q_{i-1}^{max} \tag{15}$$

For uncontrolled on-ramps, (7) is replaced with:

$$r_i(k) = d_i(k), \quad 0 \le r_i(k) \tag{16}$$

And, for controlled on-ramps, (8) is replaced with::

$$r_i(k) \le l_i(k) + d_i(k), \quad 0 \le r_i(k) \le r_i^{C,max} \tag{17}$$

In summary, (1)-(5), and (9)–(17) describe the second version of ACTM.

Version 3: The Extended ACTM The difference between this version presented in Ferrara et al. (2018) and the original ACTM version presented in (Gomes and Horowitz (2006)), named version 1 here, is how this version handles the merge between the on-ramp and mainstream cells. This version distinguishes between the flow rate equations of the free flow and congested case when on-ramp flow is merging to the mainstream flow. To do so, let's first introduce the demand and supply functions. The mainstream cell demand $D_{i-1}(k)$ is the flow that cell $i-1$ could send to the next cell i and the mainstream cell supply $S_i(k)$ is the flow that cell i could receive from cell $i-1$.

$$D_{i-1}(k) = \min\{(1-\beta_{i-1}(k))v_{i-1}\rho_{i-1}(k), q_{i-1}^{max}\} \tag{18}$$

$$S_i(k) = \min\{w_i(\rho_i^{max} - \rho_i(k)), q_i^{max}\} \tag{19}$$

Also, the on-ramp demand $D_i^{ramp}(k)$ is the flow that can be sent from the on-ramp into cell i.
For uncontrolled on-ramps:

$$D_i^{ramp}(k) = \min\{d_i(k) + \frac{l_i(k)}{T}, r_i^{max}\} \tag{20}$$

For controlled on-ramps:

$$D_i^{ramp}(k) = \min\{d_i(k) + \frac{l_i(k)}{T}, r_i^C(k), r_i^{max}\} \tag{21}$$

The merge between the on-ramp and the mainstream is analogous to the merge of two generic cells. Two cases must be distinguished, corresponding, respectively, to free-flow and congested conditions:
If $D_{i-1}(k) + D_i^{ramp}(k) \leq S_i(k)$ (free-flow case), then

$$\begin{aligned} \phi_i(k) &= D_{i-1}(k) \\ r_i(k) &= D_i^{ramp}(k) \end{aligned} \tag{22}$$

If $D_{i-1}(k) + D_i^{ramp}(k) \geq S_i(k)$ (congested Case), then

$$\begin{aligned} \phi_i(k) &= \text{mid}\{D_{i-1}(k), S_i(k) - D_i^{ramp}(k), p_i S_i(k)\} \\ r_i(k) &= \text{mid}\{D_i^{ramp}(k), S_i(k) - D_{i-1}(k), p_i^{ramp} S_i(k)\} \end{aligned} \tag{23}$$

where the function mid returns the middle value. The parameters p_i and p_i^{ramp} model, respectively, the priority of the mainstream flow and the on-ramp flow in the merge and $p_i^{ramp} + p_i = 1$.

In summary, (1)-(5), (9)-(12), and (18)-(23) describe the third version of the ACTM. Note that, the split ratios, i.e. $\beta_i(k)$, the demand in the cell before the first one, i.e. $D_0(k)$, and the supply of the cell after the last one, i.e. $S_{N+1}(k)$, and the flows accessing the on-ramp queues, i.e. $d_i(k)$ are the boundary conditions in this version.

It should be added here that all the three versions explained up to this point represent the necessary equations to model a freeway *stretch*. In order to model a freeway *network*, it is necessary to also add the merge and diverge models. Detailed explanations can be found in Ferrara et al. (2018). Since, these models are the same for all the versions stated above, and having them here would not affect the goal of this study, their details are not provided and interested readers are motivated to study the main reference.

3. RAMP METERING CONTROL

Ramp metering is achieved by placing traffic signals at on-ramps to control the flow rate at which vehicles enter the freeway. The ramp metering controller computes the metering rate to be applied. This paper applies the feedback local RM strategy PI-ALINEA proposed by Wang et al. (2014) which is an extension of ALINEA developed by Papageorgiou et al. (1991). According to the stability analysis of the closed-loop RM system reported by Wang et al. (2014), it can be stated that PI-ALINEA is able to guarantee a better control performance than ALINEA. PI-ALINEA is basically a PI-type controller in which the metering rate is given by

$$r_i^C(k) = r_i^C(k-1) + K_R[\rho_i^* - \rho_i(k)] - K_P[\rho_i(k) - \rho_i(k-1)] \tag{24}$$

where the flow that can enter section i of a freeway from the on-ramp of cell i during time interval $[kT, (k+1)T)$ is shown by $r_i^C(k)$. In case, the main objective of the traffic controller is to reduce congestion and to maximize the throughput, a good choice for the set-point is $\rho_i^* = \rho_i^{cr}$.

4. FINITE HORIZON OPTIMAL CONTROL PROBLEMS (FHOCPS)

The main objective of traffic control is to improve the network performance. However, network performance can be interpreted in many ways, and for every interpretation a different optimization problem can be formulated. To achieve the goal of this study, four FHOCPs will be proposed in this section and the above-mentioned ACTM versions will play the role of the underlying model in these optimization control problems. In section 4.1, the cost functions considered for these problems will be explained and in section 4.2, the formulation of these FHOCPs will be presented in a compact form.

4.1 Cost functions

In this section, the definitions of several cost functions will be provided. In the formulation of FHOCPs presented in this section, a linear combination of these cost functions will make the final objective of each problem.

The most frequently used objective is to minimize the total time that all vehicles spend in the network (i.e., the Total Time Spent or TTS). Another advantage of the TTS is that it can easily be calculated for macroscopic models. Basically, the TTS is the time spent by all vehicles in the network (i.e., the total travel time or TTT), including the waiting time experienced at origins (i.e., the total waiting time or TWT). In other words, $TTS = TTT + TWT$.

$$J_1 = J_{TTS} = T \sum_{k=0}^{K-1} [\sum_{i=1}^{N} \rho_i(k) L_i \lambda_i + \sum_{i=1}^{N} l_i(k)] \tag{25}$$

The second objective function applied here is to maximize the sum of the traffic flows going through all sections and on-ramps. This objective function is also called the Total Travel Distance (TTD) since it is the total distance (veh mi) covered by all the vehicles in the considered time horizon.

$$J_2 = J_{TTD} = T \sum_{k=0}^{K-1} [\sum_{i=1}^{N} \phi_i(k) L_i + \sum_{i=1}^{N} r_i(k) L_i] \tag{26}$$

Another term that is often used in the objective function of traffic management problems is a term that penalizes control signal variations. This terms helps to suppress the high-frequency oscillations of the control trajectories. Since here RM provides the control variable, the following term is penalizing the RM control variable:

$$J_3 = J_{r_i^C} = T \sum_{k=0}^{K-1} \sum_{i=1}^{N} [r_i^C(k) - r_i^C(k-1)]^2 \tag{27}$$

Also, the maximum ramp queue constraints may be taken into account via the introduction of a penalty term in the cost criterion penalizing queue lengths larger than l_{max}, the maximum admissible queue for origin i.

$$J_4 = J_{l_i} = T \sum_{k=0}^{K-1} \sum_{i=1}^{N} [\max\{0, l_i(k) - l_{max}\}]^2 \tag{28}$$

Optimizing TTS and TTD are the main objective of this study and the contribution of the two penalty terms to the total cost criterion is very small as these two only penalize control signal variations. Therefore, they are not used as separate costs functions. For a traffic problem, a trade-off has to be made between the partial objective functions $J_i(k)$, $i = \{1, 2, 3, 4\}$, which can be expressed by combining the objective functions into one objective function:

$$J_{total} = \sum_i \alpha_i J_i(k) \tag{29}$$

where α_i are appropriately chosen weights to express the trade-off between the several partial objective functions and in each problem $\sum_i \alpha_i = 1$.

4.2 Problem Formulation of FHOCPs

In this section, four FHOCPs will be presented where the control strategy in all of them is the PI-ALINEA RM control. The difference between these problems is on the cost function and the version of the ACTM used as the model. For two of the problems a linear combination of TTS and TTD is used and for the other two problems, the two penalty terms are also considered. Regarding the ACTM version used, version 1 of the ACTM has the underlying equations used in the other two versions. As a result, it will not be used as a separate model for the simulation phase of this study. For FHOPC 1 and 2, the extended ACTM and for FHOPC 3 and 4, the linear approximation of ACTM described in section 2 is used. The formulation of the four FHOCPs proposed in this study is provided in a compact form as follows:

FHOCP 1:
Cost function:

$$\min_{r_i^C} \alpha_1 J_1 - \alpha_2 J_2 \tag{30}$$

Subject to:
Equations (1)-(5), (9)-(12), and (18)-(24).

FHOCP 2:
Cost function:

$$\min_{r_i^C} \alpha_1 J_1 - \alpha_2 J_2 + \alpha_3 J_3 + \alpha_4 J_4 \tag{31}$$

Subject to:
Equations (1)-(5), (9)-(12), and (18)-(24).

FHOCP 3:
Cost function:

$$\min_{r_i^C} \alpha_1 J_1 - \alpha_2 J_2 \tag{32}$$

Subject to:
Equations (1)-(5), (9)-(12), (13)-(17), and (24).

FHOCP 4:
Cost function:

$$\min_{r_i^C} \alpha_1 J_1 - \alpha_2 J_2 + \alpha_3 J_3 + \alpha_4 J_4 \tag{33}$$

Subject to:
Equations (1)-(5), (9)-(12), (13)-(17), and (24).

In the total cost function of each problem, every partial function with a positive sign will be minimized and every other one with a negative sign will be maximized.

5. SIMULATION RESULTS AND ANALYSIS

5.1 Case study and model parameters

Simulation is performed for the network shown in Fig. 2 with two origins ($o1$ and $o2$), two controlled on-ramps ($o3$ and $o4$), 12 mainline links ($m1$ through $m12$) and two destinations ($d1$ and $d2$). One assumption about the network is that the proportion of turns at every junction, i.e. the split ratios $\beta_i(k)$, are fixed and known in advance.

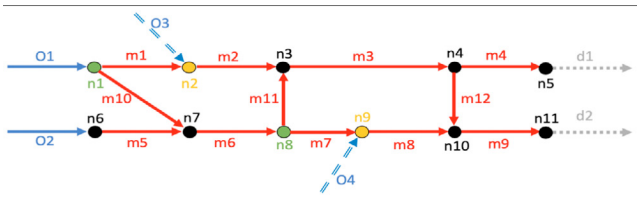

Fig. 2. The hypothetical network

Also, it is assumed that the behavior of all the links can be described by a pre-known fundamental diagram with the parameters shown in table 2 adopted from Gomes et al. (2008):

Table 2. Model Parameters

Symbol	Value	Unit/Range
Period T	0.5	min
Length L_i	1	mi
v_i	0.5	length/period
w_i	0.16	length/period
$\bar{n}_i$	160	veh/length
n_i^c	40	veh/length
$\bar{f}_i$	20	veh/period

5.2 The Demand Profiles

The simulation horizon of 5 hours is considered by choosing the time horizon of $K = 600$ time steps and the simulation period of $T = 0.5$ minute ($K*T = 300$ minute). For the origin links, two different types of demand profiles are applied: 1) the stationary, and 2) the time varying. Also, in order to approximate an empty final condition (Gomes and Horowitz (2006)), a imaginary "cool down" period is considered at $K = 450$ till the end of the time horizon, in which all demands are set to zero. The demand profiles are shown in Fig. 3. It is important to notice that although the time-varying demand is changing at different time steps, however, the max values for each of the four demand functions are chosen to be fixed to the values of demand in the stationary demand profile. For example, the demand of origin 2 is equal to 9 veh/0.5 min in the stationary demand case between $k = 0$ to $k = 450$. On the other hand, in the time-varying case, this function also has the max value of 9 veh/0.5 min between $k = 100$ to $k = 400$. Also, all demand values has the min value of zero in the cool-down period. This holds true for all the four demand functions. The reason behind these choices are due to the fact that similar max and min values makes it easier to compare and analyze the solutions based on these two different demand patterns.

5.3 Equilibrium State of the Network

According to Gomes et al. (2008), for each stationary demand vector $d(k) = (d0, ..., d_M)$, there exists a unique equilibrium flow rate $q(k) = (q_0, ..., q_N)$ and density vector $\rho(k) = (\rho_0, ..., \rho_N)$. Detailed explanation on the calculation of these vectors is concisely explained in Gomes et al. (2008). Table 3 shows the theoretical equilibrium flow vector for the mainline links of this network based on the stationary demand vector shown in Fig. 3. Knowing this theoretical flow vector provides an insight on what should be expected to be seen in the simulation results.

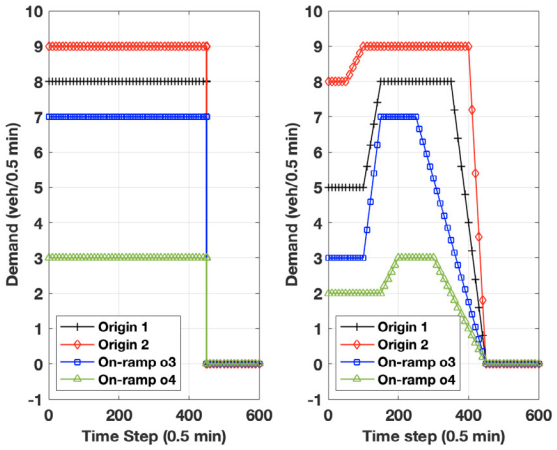

Fig. 3. The demand profiles (Left: The stationary demand profile, Right: The time-varying demand profile)

Although based on Gomes et al. (2008), the equilibrium state of the network can only be computed for the case of having stationary demand profiles, however, this information, if available, will help to analyze the behavior of models even for the case of applying time-varying demand profile. It can be assumed that at each time step, the values of the demand functions are kept constant between the time interval $[kT, (k+1)T)$. Based on this assumption, the equilibrium flow vector for the time-varying case was also computed with the same method applied before. However, in this case, this vector cannot be simply showed in a table like table 3 as the flow values are time-varying through the whole simulation horizon. Still, this information could help to analyze the performance of the FHOCPs in the time varying case. Further explanations are provided in section 5.4.

Table 3. Theoretical equilibrium flow rate (veh/0.5 min) vector

Link Number	**1**	**2**	**3**	**4**	**5**	**6**
Flow rate	4.8	11.8	15.46	9.27	9	12.2
Link Number	**7**	**8**	**9**	**10**	**11**	**12**
Flow rate	8.54	11.54	17.72	3.2	3.66	6.18

5.4 Simulation Results

The results of the simulation for the demand profiles of section 5.2 and the FHOCPs of section 4.2 are provided in this section. The FHOCPs were solved with Yalmip, the modeling and optimization language offered by Löfberg (2004), and the GURUBI non-commercial optimization solver via the interface of MATLAB. The simulations were performed on a device with 2.9 GHz Dual-core Intel Core i5 CPU with 8GB RAM.

Figures 4 and 5 show the boxplot of the mainline link flow rates (veh/0.5 min) with the stationary and time-varying demand profiles, respectively. With a general glance, it can be seen that in both figures, all four problems are showing similar behaviors for the evaluation of the mainline flow rates. In Fig. 4, the top edge and the central mark of each box are in the same position and it is fixed at the value equal to theoretical flow of that link based on table 3. In other words, all four FHOCPs are able to reach the equilibrium state of the network in case of the stationary demand. In Fig. 5, the top edge is at the same position as the top edge in Fig. 4, however, the central mark is at a lower level. This matches the expectations in the sense that as the demand is changing, the flow rate values can not converge to a constant value. However, the top and bottom edge of each box are at the same position between these two figures for all the links.

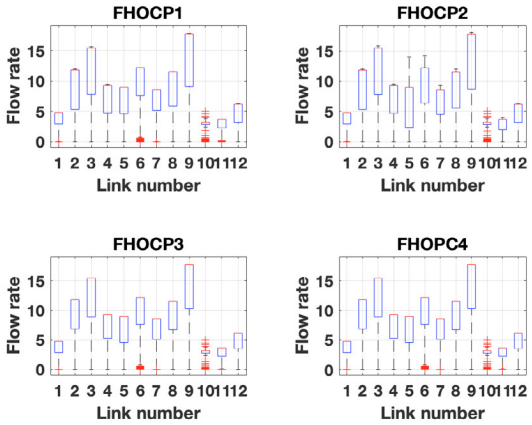

Fig. 4. Boxplot of the mainline link flow rates (veh/0.5 min) with the stationary demand profile

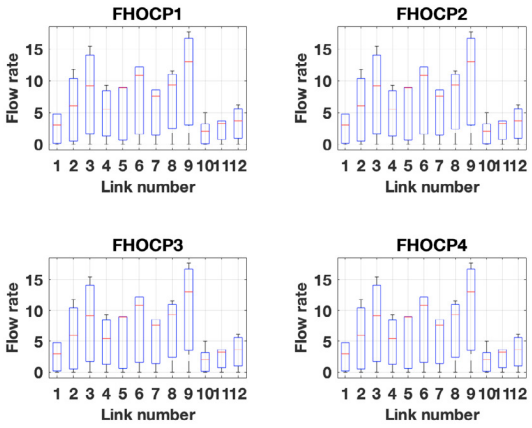

Fig. 5. Boxplot of the mainline link flow rates (veh/0.5 min) with the time-varying demand profile

A method to compare the evolution of flow rates in these optimal problems, under the two defined demand profiles, is to compute the root-mean-square error (RMSE) of the flow rate values comparing to their theoretical equilibrium values. Basically, RMSE is a frequently used measure of the differences between values (sample or population values) predicted by a model and the values observed. Table 4 summarizes the RMSE values for each problem with the two demand profiles applied. As it can be seen, overall, the FHOCPs show less error if the demand pattern is stationary, indicating that the optimal control problems demonstrated higher accuracy in converging to the equilibrium state of the network. However, the mean value of the RMSE of the second case has also a fairly low

value, proving that even with the time-varying demand profiles applied, the FHOCPs can provide an acceptable performance. Also comparing performance of FHOCPs with different underlying ACTM versions, on average, the problems with the extended ACTM version are showing slightly better efficiencies.

Table 4. Comparison of the RMSE of the flow rate values

Problem	RMSE	
	Stationary	Time-varying
FHOCP 1	1.7224	2.5344
FHOCP 2	2.3112	2.2070
FHOCP 3	2.2949	2.9585
FHOCP 4	2.0179	2.8940

The analysis continues by providing the evolution of flow rate values of the network by simply adding the flow rate of all the mainline links, as shown in Fig. 6. Based on table 3, the total sum of the link flow rates at the steady state is expected to be equal to 113.37 veh/0.5 min. This matches perfectly with the experimental maximum value of the network flow rate as seen in Fig. 6 in both cases. A very considerable point to mention is the difference between the fluctuations of the flow rate in each problem. FHOCP 1 (blue color) is showing much more fluctuations comparing to FHOCP 2 (red color) as the cost function of FHOCP 2 has the two penalty terms explained in section 4.1 and they are successfully suppressing the high-frequency oscillations of the control trajectories. Same can be seen between the performance of FHOCP 3 and 4 where less oscillations are seen in the performance of FHOCP 4 due to the presence of the penalty terms in its cost function.

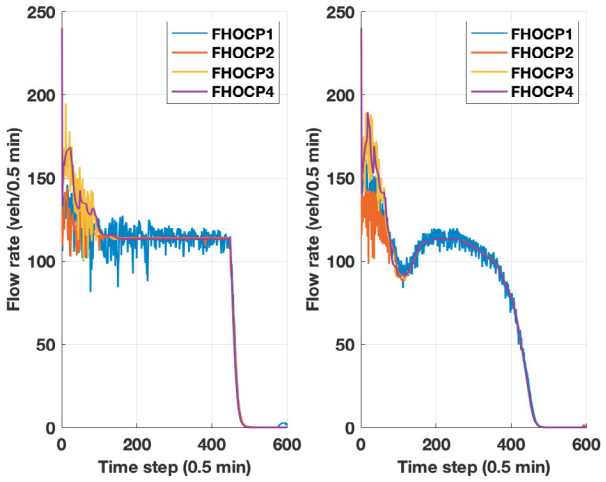

Fig. 6. Network flow rates (veh/0.5 min) (Left: The stationary demand profile, Right: The time-varying demand profile)

The evolution of the ramp metering variables are also investigated here. Basically, the expectation is that the control applied to the on-ramps can satisfy the requirements of the network while considering the external demand of the on-ramps by not imposing too much waiting time to the vehicles on the on-ramps. As a result, a propor RM variable basically should replicate the overall demand pattern of that on-ramp. As an example, Fig. 7 and 8 show the RM variable of on-ramp *o*4. It can be easily seen that in both figures, all four problems are showing a behavior similar to the demand function of this on-ramp as seen in Fig. 3 (in green color with triangle marker). The interesting point is the reduction of oscillations between FHOCP 1 and 2 and also between FHOCP 3 and 4 which clearly represent the impacts of the RM penalty terms in the cost function of FHOCP 2 and 4.

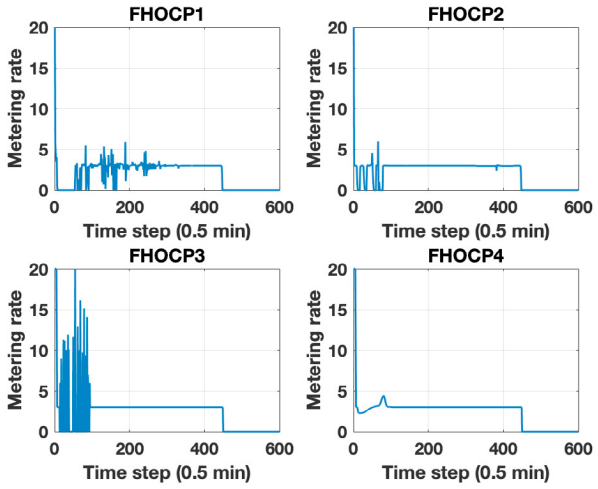

Fig. 7. Metering rate of on-ramp o4 (veh/0.5 min) with the stationary demand profile

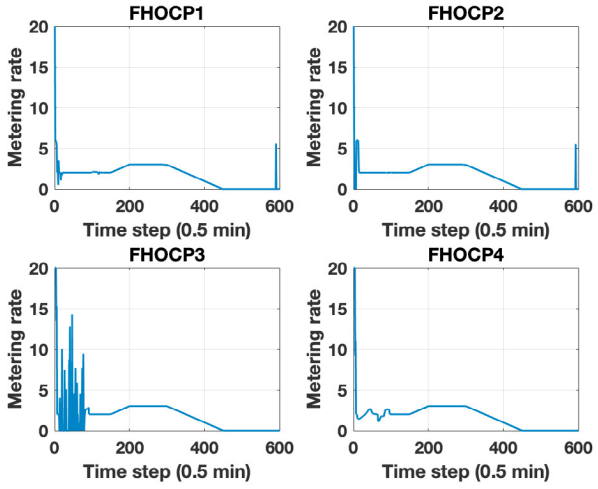

Fig. 8. Metering rate of on-ramp o4 (veh/0.5 min) with the time-varying demand profile

5.5 Analysis of the Computation Times

To complete the analysis, computation time was also considered as an additional performance index. Table 5 provides the computation time of all problems under the two demand patterns applied. FHOCPs 1 and 2 had considerable higher computation times comparing to FHOCPs 3 and 4 with respect to both demand patterns. The reason is the complexity of extended ACTM, and to be more precise, due to the presence of *min* function in its equations. Also, FHOCPs 2 and 4 also had higher computation times in comparison with FHOCPs 1 and 3

because of the presence of the two penalty terms in their cost functions. To summarize, the extended CTM and the cost functions with penalty terms can significantly increase the computation times.

Table 5. Comparison of the computation times

Problem	Computation Time (sec)	
	Stationary	Time-varying
FHOCP 1	165.3497	78.6285
FHOCP 2	324.0605	89.8481
FHOCP 3	11.4909	12.9580
FHOCP 4	28.0055	34.4486

6. CONCLUSION

This paper provides a thorough analysis over the performance of different ACTM versions used as the underlying traffic flow models for the proposed FHOCPs. The FHOCPs had different cost functions, but for all of them, the PI-ALINEA RM metering control was applied. All 4 FHOCPs had promising performances regarding the convergence of flow rates to the theoretical equilibrium flow vector, and the metering rate of on-ramps and how they can follow the changes of origin demands. Simulation results have shown that using the linear relaxed version of the ACTM is motivated by computational consequences. The extended ACTM can show better capabilities in modeling the traffic flow variables and responding to the traffic control applied. However, it is complicated, and therefore it decreases the computational efficiency of the optimization scheme.

REFERENCES

Ahmed, A., Ukkusuri, S.V., Mirza, S.R., and Hassan, A. (2019). Width-based cell transmission model for heterogeneous and undisciplined traffic streams. *Transportation research record*, 2673(5), 682–692.

Canudas-de Wit, C. and Ferrara, A. (2016). A variable-length cell road traffic model: Application to ring road speed limit optimization. In *2016 IEEE 55th Conference on Decision and Control (CDC)*, 6745–6752. IEEE.

Chen, R., Zhang, T., and Levin, M.W. (2020). Effects of variable speed limit on energy consumption with autonomous vehicles on urban roads using modified cell-transmission model. *Journal of Transportation Engineering, Part A: Systems*, 146(7), 04020049.

Daganzo, C. (1993). The cell transmission model part i: a simple dynamic representation of higheay traffic. *PATH Report, 93-0409*, 3.

Daganzo, C.F. (1994). The cell transmission model: A dynamic representation of highway traffic consistent with the hydrodynamic theory. *Transportation research part B: methodological*, 28(4), 269–287.

Daganzo, C.F. (1995). The cell transmission model, part ii: network traffic. *Transportation Research Part B: Methodological*, 29(2), 79–93.

Daganzo, C.F. (1999). The lagged cell-transmission model.

Ferrara, A., Nai Oleari, A., Sacone, S., and Siri, S. (2015). Freeways as systems of systems: A distributed model predictive control scheme. *IEEE Systems Journal*, 9(1), 312–323. doi:10.1109/JSYST.2014.2317931.

Ferrara, A., Sacone, S., and Siri, S. (2015). Event-triggered model predictive schemes for freeway traffic control. *Transportation Research Part C: Emerging Technologies*, 58, 554–567.

Ferrara, A., Sacone, S., and Siri, S. (2018). *Freeway traffic modelling and control*. Springer.

Gomes, G. and Horowitz, R. (2006). Optimal freeway ramp metering using the asymmetric cell transmission model. *Transportation Research Part C: Emerging Technologies*, 14(4), 244–262.

Gomes, G., Horowitz, R., Kurzhanskiy, A.A., Varaiya, P., and Kwon, J. (2008). Behavior of the cell transmission model and effectiveness of ramp metering. *Transportation Research Part C: Emerging Technologies*, 16(4), 485–513.

Lighthill, M.J. and Whitham, G.B. (1955). On kinematic waves i. flood movement in long rivers. *Proceedings of the Royal Society of London. Series A. Mathematical and Physical Sciences*, 229(1178), 281–316.

Löfberg, J. (2004). Yalmip : A toolbox for modeling and optimization in matlab. In *In Proceedings of the CACSD Conference*. Taipei, Taiwan.

Mayakuntla, S.K. and Verma, A. (2019). Cell transmission modeling of heterogeneous disordered traffic. *Journal of Transportation Engineering, Part A: Systems*, 145(7), 04019027.

Morbidi, F., Ojeda, L.L., De Wit, C.C., and Bellicot, I. (2014). A new robust approach for highway traffic density estimation. In *2014 European Control Conference (ECC)*, 2575–2580. IEEE.

Muñoz, L., Sun, X., Horowitz, R., and Alvarez, L. (2003). Traffic density estimation with the cell transmission model. In *Proceedings of the 2003 American Control Conference, 2003.*, volume 5, 3750–3755. IEEE.

Muralidharan, A., Dervisoglu, G., and Horowitz, R. (2009). Freeway traffic flow simulation using the link node cell transmission model. In *2009 American Control Conference*, 2916–2921. IEEE.

Papageorgiou, M., Hadj-Salem, H., Blosseville, J.M., et al. (1991). Alinea: A local feedback control law for on-ramp metering. *Transportation Research Record*, 1320(1), 58–67.

Qin, Y. and Wang, H. (2019). Cell transmission model for mixed traffic flow with connected and autonomous vehicles. *Journal of Transportation Engineering, Part A: Systems*, 145(5), 04019014.

Roncoli, C., Papageorgiou, M., and Papamichail, I. (2015). Traffic flow optimisation in presence of vehicle automation and communication systems–part i: A first-order multi-lane model for motorway traffic. *Transportation Research Part C: Emerging Technologies*, 57, 241–259.

Srivastava, A. and Geroliminis, N. (2013). Empirical observations of capacity drop in freeway merges with ramp control and integration in a first-order model. *Transportation Research Part C: Emerging Technologies*, 30, 161–177.

Szeto, W.Y. (2008). Enhanced lagged cell-transmission model for dynamic traffic assignment. *Transportation Research Record*, 2085(1), 76–85.

Wang, Y., Kosmatopoulos, E.B., Papageorgiou, M., and Papamichail, I. (2014). Local ramp metering in the presence of a distant downstream bottleneck: Theoretical analysis and simulation study. *IEEE Transactions on Intelligent Transportation Systems*, 15(5), 2024–2039.